Article

Defluorination of Organofluorine Compounds Using Dehalogenase Enzymes from *Delftia acidovorans* (D4B)

Sanaz Farajollahi, Nina V. Lombardo, Michael D. Crenshaw, Hao-Bo Guo, Megan E. Doherty, Tina R. Davison, Jordan J. Steel, Erin A. Almand, Vanessa A. Varaljay, Chia Suei-Hung, Peter A. Mirau, Rajiv J. Berry, Nancy Kelley-Loughnane,* and Patrick B. Dennis*

Read Online

ACCESS | Metrics & More | Article Recommendations | SI Supporting Information

ABSTRACT: Organofluorine compounds have been widely used as pharmaceuticals, agricultural pesticides, and water-resistant coatings for decades; however, these compounds are recognized as environmental pollutants. The capability of microorganisms and enzymes to defluorinate organofluorine compounds is both rare and highly desirable to facilitate environmental remediation efforts. Recently, a strain of *Delftia acidovorans* (D4B) was identified with potential biodegradation activity toward perfluoroalkyl substances (PFAS) and other organofluorine compounds. Genomic analysis found haloacid and fluoroacetate dehalogenases as enzymes associated with *Delftia acidovorans*. Here, defluorination activity of these enzymes toward different fluorinated substrates was investigated after their recombinant expression and purification from *E. coli*. Using an electrochemical fluoride probe, ^{19}F NMR, and mass spectrometry to monitor defluorination, we identified two dehalogenases, DeHa2 (a haloacid dehalogenase) and DeHa4 (a fluoroacetate dehalogenase), with activity toward mono- and difluoroacetate. Of the two dehalogenases, DeHa4 demonstrated a low pH optimum compared to DeHa2, which lost catalytic activity under acidic conditions. DeHa2 and DeHa4 are relatively small proteins, operate under aerobic conditions, and remain active for days in the presence of substrates. Significantly, while there have been many reports on dehalogenation of monofluoroacetate by dehalogenases, this study adds to the relatively small list of enzymes reported to carry out enzymatic defluorination of the more recalcitrant disubstituted carbon in an organofluorine compound. Thus, DeHa2 and DeHa4 represent organofluorine dehalogenases that may be used in the future to design and engineer robust defluorination agents for environmental remediation efforts.
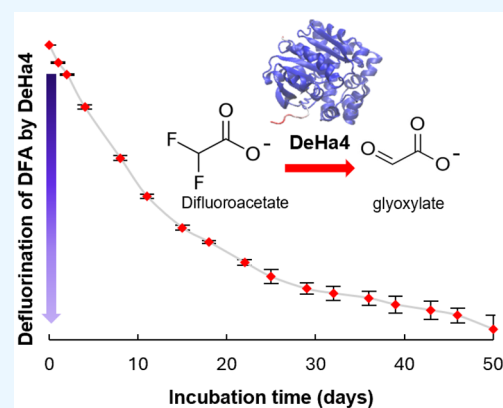
1. INTRODUCTION

Fluorinated molecules have unique physical, chemical, and biological properties, leading to distinctive roles in many diverse technologies over the last century,[1−4] beginning with the application of Freon for refrigeration in the 1930s.[1] Today 20% of pharmaceutical drugs,[5] over 50% of recent agrochemicals[6,7] and many advanced materials such as firefighting foams,[8] as well as water/oil- and wear-resistant coatings, are made with organofluorine chemicals. The ubiquitous use of organofluorine compounds has led to widespread contamination of soil and groundwater from manufacturing sites, landfills, and firefighting foam runoff, leading to increased concerns over their persistence and bioaccumulation in the environment.[4] This is especially alarming considering the known adverse effects of these compounds on human health, being linked to cancer, liver damage, decreased fertility, and increased risk of asthma and thyroid disease.[9] Because of the public health risk associated with chronic exposure to fluorochemicals, the Environmental Protection Agency (EPA) has set strict limits for the safe amounts of these chemicals in drinking water.

Destruction of organofluorine chemicals through bioremediation is highly desirable as a cheap and sustainable option; however, this method is not currently practical because enzymatic defluorination is an inefficient process that requires a better understanding of enzymatic mechanisms.[10] To date, microbial biodegradation of fluorinated compounds occurs very slowly (on a scale of weeks and months) and only for a limited number of compounds. From these microorganisms, a handful of enzyme families have been identified that can carry out dehalogenation reactions, such as the haloacid dehalogenases,[11−13] fluoroacetate dehalogenases,[6,10,14] and reductive

dehalogenases.[15] Reductive dehalogenases are metalloenzymes which are capable of defluorinating perfluoroalkyl acids (PFAAs) using a Feammox process.[15,16] However, this process is slow and requires anaerobic conditions.[16] On the other hand, both haloacid dehalogenases and fluoroacetate dehalogenases are enzymes that have catalytic activity under aerobic conditions and have been studied structurally and mechanistically in significant detail, although their dehalogenation activities have been recorded only on short-chain, partially fluorinated carboxylic acids.[6,10,11,17,18]

Fluoroacetates (FAs), including, mono (MFA)-, di (DFA)-, and trifluoroacetate (TFA) are important building blocks and intermediary reagents for the chemical synthesis of various organofluorine compounds, especially PFAS.[19] In addition, incomplete abiotic degradation of perfluoroalkyl substances can produce these short-chain fluorinated carboxylic acids as byproducts.[20] MFA is a fluorine-containing compound with high toxicity (median lethal dose of $LD_{50} = 10$ mg/kg in humans) that has been used as a pesticide in many countries.[21,22] While enzymatic defluorination of MFA has been reported by numerous enzymes,[23] increases in the degree of fluorination create recalcitrant compounds (e.g., DFA and TFA) that are not readily degradable using known dehalogenase enzymes. Therefore, understanding enzymatic FA breakdown will enable a better design of dehalogenase enzymes as a cheap, sustainable, and environmentally friendly alternative for organofluorine decontamination of soil and water.

Here, we expressed and purified a series of dehalogenase enzymes that were recently identified in *Delftia acidovorans* D4B, isolated from PFAS-contaminated soil.[24,25] Screening the purified enzymes against a panel of organofluorine substrates, we found a haloacid dehalogenase (DeHa2) and a fluoroacetate dehalogenase (DeHa4), that demonstrated degradation of both mono- and difluoroacetate (MFA and DFA). Although DeHa2 and DeHa4 displayed slower defluorination kinetics compared to other haloacid and fluoroacetate dehalogenases reported earlier for fluoroacetate dehalogenation,[26,27] the activity of DeHa4 showed both catalytic stability at long reaction times and broad pH stability—attractive features for a fluoroacetate dehalogenase with the ability to defluorinate organofluorine compounds containing disubstituted carbons. Finally, using AlphaFold2 modeling, we modeled the DeHa2 and DeHa4 active sites to better understand how fluorinated substrates interact with the two dehalogenases.

2. RESULTS AND DISCUSSION

2.1. Defluorination Profiles of the Recombinant *Delftia* Dehalogenases.
Recently, Harris et al. isolated a strain of *Delftia acidovorans*, named D4B from PFAS-contaminated soil with the potential for dehalogenation of perfluorochemicals (PFCs).[24] A draft genome analysis of strain D4B, based on two other *D. acidovorans* haloacid dehalogenases from the NCBI database (DeHa1 and DeHa2), identified three additional dehalogenase enzymes with potential to degrade organofluorine compounds.[25] Two of these additional dehalogenases are putative haloacid dehalogenases (DeHa3 and DeHa5), and one is a fluoroacetate dehalogenase (DeHa4).[25] Multisequence alignment (MSA)-based phylogenetic trees (Supplemental Figure 1A) put DeHa1 and DeHa2 in a separate branch from DeHa3 and DeHa4, while DeHa5 exists in a branch separate from the

other dehalogenases. There have been many studies on defluorination of organofluorine compounds using bacterial dehalogenases.[27,28] To better understand the relationship between these previously reported hydrolases and the ones presented in this study, WebLogo analyses of DeHa2 (as a haloacid dehalogenase) and DeHa4 (as a representative of fluoroacetate dehalogenase) were plotted with other dehalogenases in the same family (Supplemental Figures 2 and 3). The WebLogo analysis of DeHa2 (including ADE3811, POL0530, and 1ZRM) (Supplemental Figure 2) illustrates a highly conserved region around the residues involved with catalytic activity; mainly Asp, Arg, Ser, Lys, and Asp. While the WebLogo analysis of DeHa4 (including RPA1163, POL4478, POL4516, and RJO0230) (Supplemental Figure 3) illustrates conserved amino acids in the catalytic triad, namely, His, Tyr, and Asp. Together, these analyses indicate that both DeHa2 and DeHa4 from *Delftia acidovorans* (D4B) are related to other hydrolases in the same family and would likely have dehalogenase activity.

Since *Delftia acidovorans* D4B was isolated from PFAS-contaminated soil, we were interested in probing the capability of recombinantly expressed dehalogenases for their ability to defluorinate organofluorine compounds, with particular interest in the perfluorinated compounds. Thus, recombinant expression of (DeHa1−5) was performed in *E. coli* followed by purification as described in Methods. Sodium dodecyl sulfate polyacrylamide gel electrophoresis (SDS-PAGE) analysis of the purified enzymes showed successful expression and purification for DeHa1−5 with apparent molecular weights of the expressed proteins in close agreement with theoretical predictions (Figure 1). Four of the five purified enzymes
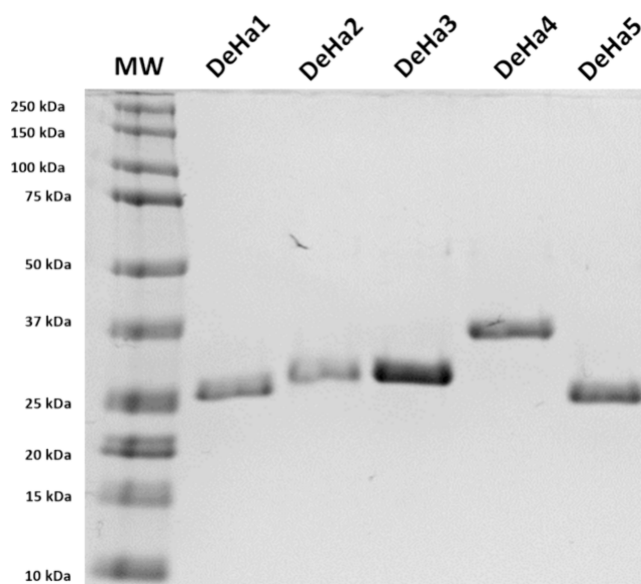

Figure 1. Coomassie blue stained SDS-PAGE gel showing *Delftia acidovorans* DeHa1−5 purified from *E. coli*. Molecular weight standards are indicated on the far left.

showed solution stability postpurification. However, DeHa3 precipitated soon after purification, precluding it from further study (data not shown). DeHa1, 2, 4, and 5 were first tested for their ability to defluorinate perfluorooctanoic acid (PFOA), an often-studied member of the PFAS family. After the incubation of each DeHa enzyme with PFOA, fluoride release was measured using a fluoride probe or ^{19}F NMR (see
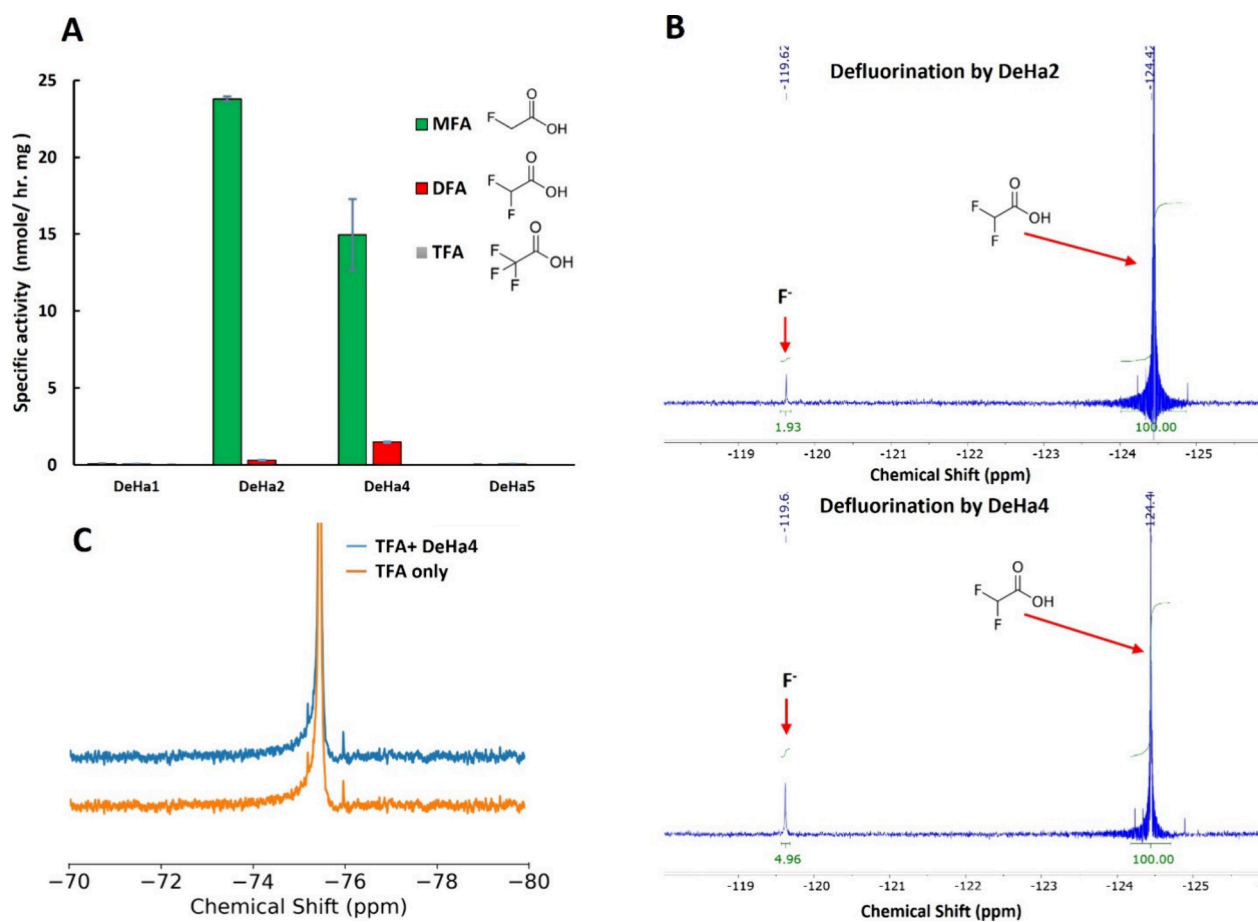
Figure 2. (A) Dehalogenation activity of DeHa1, 2, 4 and 5 enzymes evaluated using a fluoride probe after 18 h of incubation with fluoroacetate substrates (MFA, DFA, TFA) at 37 °C. (B) ^{19}F NMR analysis of DFA dehalogenation using recombinant DeHa2 (top spectrum) and DeHa4 (bottom spectrum) dehalogenases. (C) ^{19}F NMR study of TFA with and without incubation with DeHa4.

Methods). However, even after extensive incubation with the PFOA substrate (250 μg of enzyme for 7 days at 37 °C), no fluoride release was measured with any of the recombinant dehalogenases (data not shown).

Next, we systematically tested the ability of the recombinant dehalogenases to defluorinate short-chain substrates with differing degrees of fluorination. Monofluoroacetic acid (MFA) is the shortest fluorocarboxylic acid substrate that has been shown to be defluorinated by both haloacid dehalogenase and fluoroacetate dehalogenase.[13] Therefore, three short-chain organofluorine compounds, monofluoroacetate (MFA), difluoroacetate (DFA), and trifluoroacetate (TFA), were assayed with the purified dehalogenases to test their defluorination activity. Defluorination activities of DeHa1, 2, 4, and 5 were first evaluated using the fluoride ion probe. Of the four potential dehalogenases, only DeHa2 and 4 (a haloacid dehalogenase and a fluoroacetate dehalogenase, respectively) demonstrated defluorination of MFA, with DeHa2 showing higher rates of catalytic dehalogenation than DeHa4 (Figure 2A). When difluorinated DFA was used as a substrate, again only DeHa2 and 4 demonstrated defluorination activity, although both enzymes were significantly less active against DFA than MFA. It is not surprising that the defluorination rate is dramatically decreased with DFA as a substrate, since C−F bond strength rises with increasing fluorine substitution on a particular carbon.[6] In contrast to what was observed with the defluorination of MFA,

DeHa4 defluorinated DFA at a higher rate than that of DeHa2. These results are noteworthy, since defluorination of the more recalcitrant substrate, DFA, by dehalogenases has only been reported recently, in two other studies.[6,28] It should also be noted that the specific activities observed with DeHa2 and 4 are significantly lower than those reported earlier for other haloacid and fluoroacetate dehalogenases. For MFA, enzymes from both families have specific activities reported in the nmol min^{-1} mg^{-1} range, with some fluoroacetate dehalogenases having specific activities in the μg min^{-1} mg^{-1} range.[28,29] Therefore, although they demonstrate slower defluorination kinetics than previously reported dehalogenases, DeHa2 and 4 can be added to a small list of dehalogenases with the ability to defluorinate disubstituted carbons.

The reaction mixtures of DFA in the presence of DeHa2 and 4 were further analyzed using ^{19}F NMR to characterize the defluorination reaction products (Figure 2B). Interestingly, we only identified peak signals associated with the DFA substrate and the released fluoride, with no detection of a mono-fluorinated product, indicating that after the first carbon−fluorine bond is cleaved, the second fluorine bond cleaves rapidly such that no monofluorinated product accumulates. This also indicates that the rate-limiting step for defluorination of DFA by DeHa2 and 4 is removal of the first fluorine, with the monofluorinated product likely remaining in the active site of enzyme. The final product of enzymatic defluorination of DFA has been well characterized and identified as glyoxylate.[28]
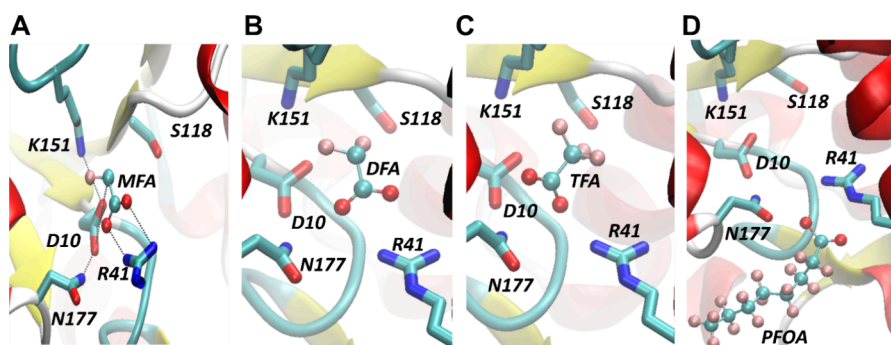
Figure 3. Binding of MFA (A), DFA (B), TFA (C), or PFOA (D) in DeHa2. Structures are constructed by AutoDock Smina. The active site residues of the protein are shown in sticks, and the ligand (MFA) is shown in sticks and spheres, with C in cyan, O in red, N in blue, and F in pink.

Figure 4. Binding of MFA (A), DFA (B), and TFA (C) in DeHa4. Structures are constructed by AutoDock Smina. The active site residues of the protein are shown in sticks, and the ligand (MFA) is shown in sticks and spheres, with C in cyan, O in red, N in blue, and F in pink.
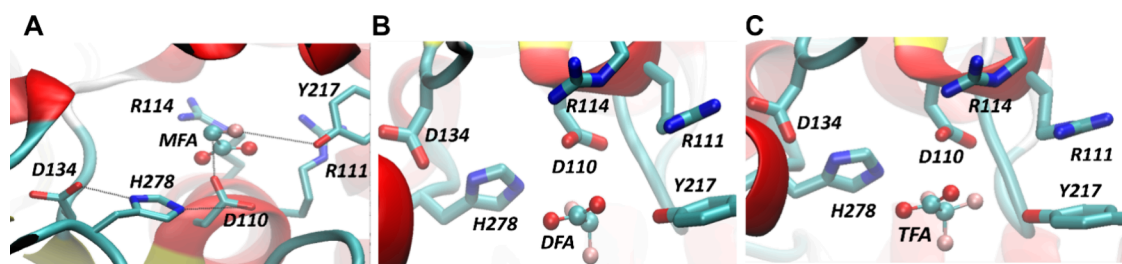
Using mass spectrometry, we confirmed the presence of glyoxylate in the reaction mixture of DFA and DeHa4 (Supplemental Figure 4) as a product of the dehalogenase activity.

Fluoroacetate dehalogenase catalyzes fluorine−carbon bond cleavage through four successive steps, (I) C−F bond activation, (II) nucleophilic attack, (III) C−O bond cleavage, and (IV) proton transfer leading to a glycolate reaction product (in the case of MFA).[6,18] Yue et al. recently proposed that the rate-limiting step for enzymatic defluorination of the monofluorinated MFA is the nucleophilic attack by aspartate and water, while for DFA and TFA, activation of the C−F bond is rate-limiting.[6] Additionally, they performed a computational analysis to compare energy barriers for catalytic defluorination of MFA, DFA, and TFA by fluoroacetate dehalogenase RPA1163, which were calculated as 11.2, 23.0, and 24.4 kcal mol^{-1}, respectively. When the trifluorinated substrate (TFA) was assayed with DeHa2 and 4, no fluoride release was detected with either enzyme by using the fluoride probe (Figure 2A). Even with longer incubation times (1 week at 37 °C) followed by ^{19}F NMR of TFA with and without DeHa4, we did not detect any difference in the spectra associated with TFA, indicating no degradation of the substrate occurred (Figure 2C).

2.2. Modeling the Active Site of *Delftia* Dehalogenases. To understand the observed differences in the defluorination activity of dehalogenases, we used AlphaFold2 (AF2) structural modeling to model the active sites of DeHa2 and DeHa4 enzymes. AF2 modeling relies on the coevolutionary information extracted from the multiple sequence alignment (MSA).[30] Therefore, the AF2 models may represent protein structures in the native states. Indeed, a recent work showed that the AF2 model of a reductive dehalogenase captures the protein structure bound with different ligands, including the PFOA substrate.[31] Here, the protein−ligand

complex models were constructed by superimposing the AF2 models with experimental X-ray crystallographic structures deposited in the Protein Data Bank.[32] The DeHa2 model was superimposed to the protein structure of L-2-haloacid dehalogenase of *Pseudomonas* sp. YL (PDB entry: 1ZRN)[33] (Figure 3), and the DeHa4 model was superimposed to the fluoroacetate dehalogenase of *Rhodopseudomonas palustris* (PDB entry: 6QHQ)[17] (Figure 4). It is worth noting that the active site residues in DeHa2 and DeHa4 are fully conserved with the respective proteins used for superimposing (Supplemental Figures 5 and 6). Here, we show that the AF2 models also possess the proper binding pockets for MFA as a substrate within the active sites of both DeHa2 and DeHa4 (Figures 3A and 4A).

To gain insights into enzyme−ligand complexation, comparative models were constructed looking at binding of different substrates (MFA, DFA, TFA, and PFOA) to the active sites of both DeHa2 and DeHa4 (Figures 3 and 4, respectively). MFA binding to DeHa2 and 4 is shown for the highest binding free energies of −3.5 and −2.3 kcal/mol, respectively (Figures 3A and 4A). For DeHa2, the docking studies show that MFA, DFA, and TFA bind to the same pocket within the active site with little change in binding free energies for DFA and TFA (−4.0 kcal/mol for each). Both MFA and DFA are oriented the same within the active site, with Arg41 interacting with the substrate carboxylate and Asp10 positioned for nucleophilic attack of the fluorinated carbon (Figure 3A,B). In contrast, TFA is tilted clockwise within the binding pocket and is not well-positioned for catalysis, suggesting that the addition of the third fluorine decreases the ability of TFA to effectively bind the active site of DeHa2 (Figure 3C). In contrast, docking studies with DeHa4 indicate the same active site orientation for MFA, DFA, and TFA (Figure 4A−C, respectively), showing the expected active site side chain interactions with the substrate and very similar
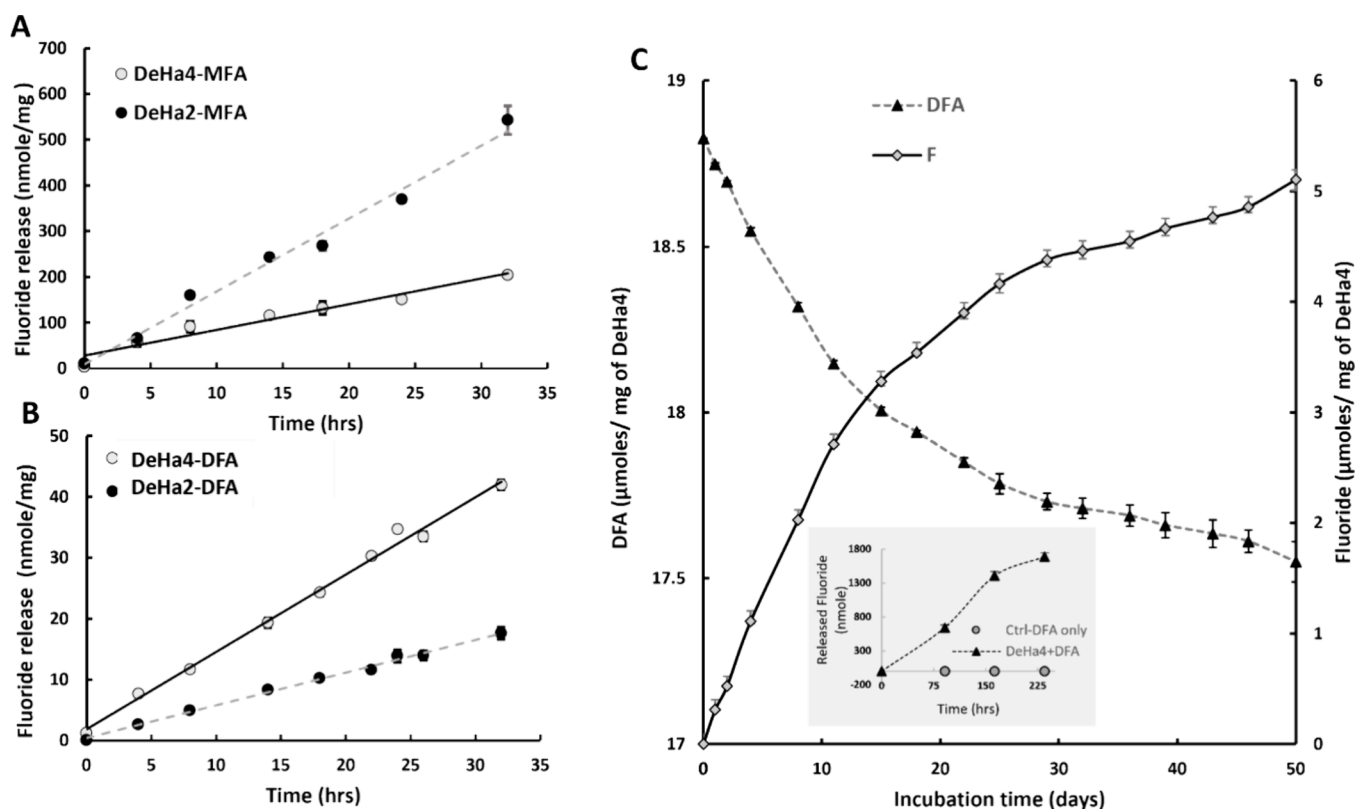
Figure 5. Time course analysis of fluoride release from MFA (A) or DFA (B) by DeHa2 and 4, respectively. (C) Long-term time course study of DFA dehalogenation, incubated with DeHa4 at 40 °C for 50 days, measured by ^{19}F NMR. The substrate (DFA) conversion is shown as a dotted line, and the fluoride production is shown as a solid line for average of 3 independent reactions. The inset is the long-term dehalogenation study measured with fluoride probe (triangles), including the buffer control (DFA only, circles).

Table 1. Kinetic Parameters of DeHa2 and DeHa4 with MFA and DFA as Substrates

enzyme	substrate	pH	K_m (mM)	V_{max} (nmol h^{-1})	K_{cat} (h^{-1})	K_{cat}/K_m (h^{-1} mM^{-1})	replicate
DeHa2	MFA	7	5.47 ± 1.54	26.6 ± 3.75	3.07 ± 0.43	0.65 ± 0.08	4
DeHa2	DFA	7	27.55 ± 1.51	2.53 ± 0.1	0.3 ± 0.01	0.011 ± 0.0002	4
DeHa4	MFA	7	2.19 ± 0.37	5.14 ± 0.54	0.77 ± 0.08	0.38 ± 0.04	6
DeHa4	DFA	7	39 ± 2.36	5.92 ± 0.82	0.74 ± 0.02	0.019 ± 0.001	5
DeHa4	MFA	6	11.55 ± 5.2	32.1 ± 12.2	4.78 ± 1.82	0.7 ± 0.16	4
DeHa4	DFA	6	11.02 ± 0.7	4.69 ± 0.2	0.7 ± 0.03	0.065 ± 0.005	4

predicted binding free energies (−2.3, −2.4, and −1.8 kcal/mol, respectively), suggesting that progressive fluorination has little impact on substrate binding to the DeHa4 active site. Finally, PFOA docks in a region outside of the binding pocket of DeHa2 with a predicted binding free energy of −3.8 kcal/mol (Figure 3D). However, PFOA was not predicted to bind to DeHa4, with a calculated binding free energy of +13.1 kcal/mol. Therefore, the modeling is consistent with the lack of defluorination activity observed with the perfluorinated PFOA substrate using either dehalogenase.

2.3. Kinetics of Defluorination by *Delftia* Dehalogenases.
Next, time-course analyses were performed comparing the fluoride release rates of MFA and DFA by DeHa2 and DeHa4 (Figure 5). As shown in Figure 2A, DeHa2 demonstrated faster reaction kinetics compared to DeHa4 when assayed against MFA, where the DeHa2 reaction is largely linear up to 30 h (Figure 5A). This result indicates that although defluorination by DeHa2 is slow, the enzyme is stable at the relatively high temperature of 37 °C and long reaction times. When difluorinated DFA was added as a substrate, the

rate of defluorination observed with DeHa4 was linear up to 32 h (Figure 5B). Although DeHa2 was less active against DFA than DeHa4, its reaction kinetics were also linear over the time course, indicating both enzymes are stable for long reaction times.

Due to the observed reaction linearity at long incubation times, ^{19}F NMR was used to measure defluorination of DFA by DeHa4 beyond the 32 h reaction time used in the previous experiments. The use of ^{19}F NMR to measure the reaction products allowed for a long-term study without perturbation of the reaction due to sample removal. In this study, defluorination activity by DeHa4 remained linear for up to 2 weeks at 40 °C, demonstrating activity, albeit slower, for up to 50 days. The decrease in activity was not due to substrate limitation, since only ~6.7% fractional substrate conversion was obtained on day 50 of incubation with an initial DFA concentration of 50 mM (Figure 5C), well above the K_m value of DeHa4 for DFA as indicated in Table 1. A separate assay using the fluoride probe confirmed the NMR studies, showing linear DeHa4 defluorination activity up to ~7 days at 40 °C
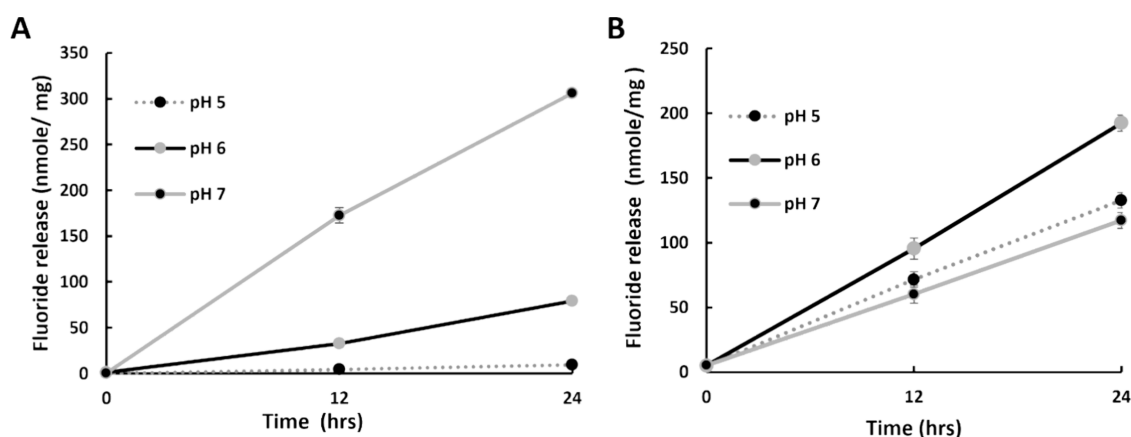
Figure 6. Time course analysis of MFA defluorination by DeHa2 (A) or DeHa4 (B) at pH 5, 6, and 7 (n = 2).

(Figure 5C, inset). These results indicate that although the reaction kinetics for the *Delftia* dehalogenases are slow, the enzymes demonstrate robust thermal stability and extraordinary linear kinetics for extended reaction times.

To give a more complete view of the dehalogenation kinetics for DeHa2 and DeHa4, a Michaelis−Menten kinetic analysis was performed on both enzymes using MFA and DFA as substrates (Table 1). The calculated K_{cat} values for DeHa2 and 4 indicated a very low turnover compared to the measured K_{cat} $(6.7 \pm 0.6 \text{ min}^{-1})$[29] of a well-studied fluoroacetate dehalogenase (RPA1163) that has defluorination activity toward both MFA and DFA.[6] RPA1163 fluoroacetate dehalogenase forms a homodimer with substrate-based allosteric regulation that entropically favors the forward reaction, where disruption of the homodimer decreased the catalytic rate by over an order of magnitude.[34] Both recombinantly expressed DeHa2 and DeHa4 were observed only as monomers by size exclusion chromatography (Supplemental Figure 7), which may explain their slow turnover compared to the RPA1163 fluoroacetate dehalogenase. As expected, the K_{cat} values decreased from monofluorinated to difluorinated substrates for both DeHa2 and DeHa4. Additionally, the K_m values measured for both enzymes decreased significantly when using MFA as a substrate compared to DFA. Using both values to derive the specificity constant, K_{cat}/K_m, further highlights that MFA is preferred as a substrate over DFA. However, with DeHa4, the K_{cat} value is not significantly changed from MFA to DFA.

2.4. pH Optima of *Delftia* Dehalogenases. The mechanisms of catalytic defluorination by fluoroacetate dehalogenases have been investigated by other researchers using crystal structures, mutagenesis, and quantum mechanics/molecular dynamics/molecular mechanics.[6,28,35−37] It is suggested that a catalytic triad of amino acids (Asp-His-Asp) is involved in this process, which initiates with C−F bond activation through nucleophilic attack of the fluoroacetate α-carbon by a negatively charged catalytic Asp to release the fluoride ion, resulting in the formation of a modified enzyme ester intermediate. Next, a water molecule activated by the catalytic His hydrolyzes the intermediate to subsequently produce glycolate.[6] It was reported that the activity of fluoroacetate dehalogenase RPA1163 drops at pHs below 7,[38] due to protonation of the catalytic His. To test the effect of low pH on the dehalogenation rates of DeHa2 and DeHa4, we performed time course analyses of MFA and DFA defluorination from pH 5 to 7. DeHa2 demonstrated a

significantly lower catalytic activity toward MFA when the pH was decreased from 7 to 6 (Figure 6A) and was nearly inactive at a pH of 5. In contrast, the activity of DeHa4 toward MFA increased when the pH was lowered from 7 to 6 and remained high when the pH was reduced to 5 (Figure 6B). A kinetic analysis of DeHa4 showed an increased K_{cat} for MFA defluorination when the pH was changed from 7 to 6 (Table 1), whereas K_{cat} for DFA defluorination was not significantly different between the two pH conditions. Consistent with the kinetics observed at pH 7, DeHa4 maintained its selectivity for MFA at pH 6, as shown by the K_{cat}/K_m values. These results indicate that both DeHa2 and DeHa4 have very different pH responses, with DeHa4 demonstrating a low pH optimum compared to those of DeHa2 and other fluoroacetate dehalogenases.

The low pH optima observed for DeHa4 contrasts with the pH profiles published for other members of the fluoroacetate dehalogenase family, where sharp decreases in activity were observed from pH 7 to 6.[36,38] Looking more closely at the active site of DeHa2, Asp10 acts as a nucleophile in the catalysis.[33] Asn177 and Lys151 form hydrogen bonds to Asp10, and Tyr12 is also present for scaffolding the MFA substrate. Therefore, the potential protonation of Asp10 could explain the sensitivity of DeHa2 to a reduction in pH (Figure 3A). For the fluoroacetate dehalogenases, it has been proposed that at low pH, protonation of the catalytic His residue would have two effects to lower defluorination activity. First, the protonated His would not act as a base catalyst for hydrolysis of the intermediate ester, and second, the protonated His, hydrogen bonded to a catalytic Asp, would block nucleophilic attack of the fluorinated carbon.[36] In the case of DeHa4, substrate binding amino acids are conserved, such as Arg111 and Arg114, which bind the acetate group, and Tyr217, which interacts with the substrate fluorine.[36] The catalytic triad amino acids are also conserved as Asp110-His278-Asp134, and the presence of these conserved residues would suggest similar pH optima for DeHa4 and other fluoroacetate dehalogenases (Figure 4A). However, pairwise sequence alignment of DeHa4 with the fluoroacetate dehalogenase RPA1163[27] (Supplemental Figure 6) indicates a 46% identity and 62% similarity between DeHa4 and RPA1163. Thus, there are sufficient differences between the two enzymes that may affect substrate binding and/or intramolecular protein interactions through hydrogen bonding, resulting in their differing pH responses. Future studies will be aimed at uncovering a mechanism for the low pH optimum of DeHa4.

3. CONCLUSION

We have studied five dehalogenases from *Delftia acidovorans*, which has previously been shown to grow in the presence of perfluorinated compounds. Of these enzymes, two demonstrated the ability to defluorinate small, fluorinated compounds, including one with a difluorinated carbon. The reaction kinetics observed with these enzymes indicate that they are inefficient. However, one of the enzymes, DeHa4, has demonstrated the ability to remain catalytically active for extended periods of time at relatively high reaction temperatures and low pH conditions, attractive properties for an enzyme aimed at bioremediation of organofluorine contaminated environments. Additionally, the ability of these dehalogenases to operate under aerobic conditions and their ability to completely defluorinate disubstituted carbons suggest DeHa2 and 4 are good starting points for the search of related dehalogenases as well as the engineering of efficient enzyme catalysts for the breakdown of perfluorinated compounds.

4. METHODS

4.1. Plasmid Design and Construction. All plasmids were constructed by subcloning gBlock DNA of each dehalogenase open reading frame (Integrated DNA Technologies) into a pET15b vector containing an amino terminal hexahistidine tag using a single cut at the NdeI site. Gibson assembly was carried out using an NEBuilder HiFi DNA Assembly kit (New England Biolabs, Inc.) as per the manufacturer's instructions. All constructed plasmids were initially transfected into DH5α competent cells for plasmid DNA production. Purified plasmid DNA was then transfected into *E. coli* BL21 DE3 cells for protein expression.

4.2. Protein Expression and Purification. The dehalogenases were expressed by inoculating 4 L of autoclaved Luria broth (LB) media with BL21 DE3 cells transfected with the individual pET15b dehalogenase plasmids followed by incubation at 37 °C with continuous shaking at 150 rpm in baffled culture flasks. Once cell cultures reached an optical density ($OD_{600\,nm}$) of 0.6−0.8, expression of the gene of interest was induced with 0.4 mM isopropyl β-D-1-thiogalactopyranoside (IPTG) for 18 h at 16 °C. Pellets from the induced overnight culture were suspended in 120 mL of lysis buffer (phosphate-buffered saline (PBS), pH 7.4, 100 μg/mL lysozyme, and 120 μL of protease inhibitor (Sigma P8849). Lysates were sonicated for 2.5 min at 40% power (15 s on, 15 s off) and centrifuged (10000 rpm, 10 min) to remove insoluble debris. Soluble fractions were then incubated with 5 mL of HisPur Cobalt Resin (ThermoFisher Scientific) for 2 h under rotation at 4 °C. Next, resin-bonded proteins were washed with wash buffer (PBS, pH 7.4, 10 mM imidazole) and then eluted with elution buffer (PBS, pH 7.4 250 mM imidazole). Proteins were then desalted on a size exclusion column (Bio-Rad's Econo-Pac 10DG Desalting Columns) into storage buffer (PBS, pH 7.4). Purified enzymes were quantified via densitometry on SDS-PAGE gels alongside BSA standards after staining with Coomassie blue R-250. All purified proteins were stored at −80 °C until use.

4.3. Size Exclusion Chromatography. Size exclusion chromatography of purified dehalogenase enzymes was performed using a Superdex 200 Increase 10/300 GL column (Cytiva 28-9909-44) on a NGC chromatography system (Bio-RAD). Molecular weight markers were purchased from Sigma, including cytochrome c (C7150), carbonic anhydrase (C7025), bovine albumin (A8531), and blue dextran (D4772). The molecular weight markers and dehalogenase enzymes were run on a size exclusion column at a flow rate of 0.5 mL/min using PBS, pH 7.4, as the running buffer. Elution of the proteins was monitored using absorbance at 280 nm.

4.4. ^{19}F NMR Characterization. The ^{19}F nuclear magnetic resonance (NMR) spectra were obtained using a Bruker Avance 400 NMR spectrometer equipped with a 5 mm broadband probe and operating at 376.55 MHz. Spectra were acquired using the following parameters: 313 K probe temperature, 3 s delay, 12 μs pulse, and 300 ppm sweep width (50 to −250 ppm). For some samples, an insert containing a solution of trifluoroacetic acid (TFA) was used as an internal standard.

4.5. Mass Spectrometry Characterization. Mass spectral data were acquired using an Agilent 1200 high-pressure liquid chromatograph (HPLC) coupled to an Agilent 6420 triple-quadrupole mass spectrometer with an electrospray ionization (ESI) source in negative ion mode with the capillary voltage set to 2500 V. The gas temperature and flow were 250 °C and 11 L/min, respectively. The nebulizer was set to a pressure of 25 psi. The HPLC was modified to remove or bypass poly(tetrafluoroethylene)-containing components with a PFC delay column placed between the pump and the autosampler. The separation column was an Agilent Zorbax Eclipse Plus C18 (2.1 mm × 100 mm, 1.8 μm) maintained at 50 °C. Solvents (A, as water; B, as methanol) contained 5 mM ammonium acetate. Ten microliters of sample was injected and eluted using a gradient of 10% B (0−0.5 min), 10−40% B (2.0 min), 40−90% B (9.5 min), and 90−100% B (0.5 min).

4.6. Defluorination Assays and Kinetic Studies. The defluorination assay was performed in 500 μL of reaction mixtures including the fluorinated substrate of interest (MFA, DFA, TFA, and PFOA) at a final concentration of 1 mM and 250 μg of dehalogenase enzymes (DeHa1−5) in a buffer at the desired pH. All the fluorinated substrates were purchased from Sigma unless otherwise indicated. Fluoroacetic acid was obtained *in situ* by hydrolysis of ethyl fluoroacetate, where complete hydrolysis was confirmed by ^{19}F NMR. PBS was used as the assay buffer at pH 7.4, and citrate buffer was used for assays run at pH of 5 and 6. The reaction mixtures were agitated at 150 rpm at 37 °C for the duration of the incubation period. For fluoride release analysis, 0.5 mL of the reaction mixture was added to 5 mL of low-level TISAB and 5 mL of HPLC grade water before released fluoride was measured with a fluoride ion probe (Mettler Toledo perfection comb F⁻, Cat# 51344715) using a portable electrochemical meter (Mettler Toledo SG78-FK2 SevenGo Duo Pro, Cat# 51302622). For creation of the calibration curve, 0.5 mL of the calibration mixture, including 250 μg of dehalogenase enzyme in PBS, pH 7.4, was mixed with 5 mL of low-level TISAB and 5 mL of HPLC grade water, and then increasing concentrations of NaF were added to the mixture to obtain concentrations of 0, 1, 2, 4, 6, 10, and 20 μM. The calibration curve was expressed as mV versus NaF concentration before being fit to a second-order polynomial equation. This equation was then used to calculate fluoride release from tested samples. Kinetic parameters for DeHa2 and 4 were measured using 250 μg of enzyme in 0.5 mL of the reaction mixture including the substrate and buffer, incubated for 28 h at 37 °C, and mixed at 250 rpm. Fluoride release from each reaction mixture was measured in nmol using an electrochemical fluoride probe for various concentrations of substrates (S) namely, 0.4, 0.6, 0.8, 1,

2, and 3 mM for MFA and 10, 25, 50, 75, 100, and 120 mM for DFA. PBS was used as the assay buffer at pH 7, and citrate buffer was used for assays run at pH 6. All the experiments were run for 4−6 times independently and in multiples within each set. The amount of product converted in case of the MFA as substrate was same as the amount of fluoride release, while in terms of DFA, it was half of the measured fluoride release. Velocity (V) was calculated as converted product per hour of reaction. Lineweaver−Burke plots were graphed by plotting $1/V$ over $1/S$ and the kinetic constants (K_m, K_{cat}, and K_{cat}/K_m) were derived using the equations

$$1/V = (K_m/V_{max})(1/S) + (1/V_{max})$$

$$K_{cat} = V_{max}/[e]$$

where [e] is the concentration of the enzyme. For the dehalogenation assays, each data point was carried out in duplicate, and the number of independent experiments performed is noted in the figure legends. The average and standard deviation for each data point are a combination of all measurements from the independent experiments.

4.7. Bioinformatics and Structural Modeling. Using each of the individual DeHa sequences, we conducted the BLASTP search from the NCBI cluster NR database.[39] The mined sequences were aligned using structure-guided multiple sequence alignment by MAFFT (v7.453),[40] and the neighbor-joining algorithm was used to reconstruct the multisequence alignment (MSA)-based phylogenetic trees of each dehalogenase. WebLogo (v3.6.0)[41] was used to plot the sequence logos. The phylogenetic trees were generated using MegaX.[42]

The atomic structures of the dehalogenases DeHa1−5 were created using AlphaFold2 (AF2, V2.2.2),[30] and to understand the structure dissimilarity among these enzymes, the root-mean-square deviations (RMSDs) of all AF2 models (five for each dehalogenase) have been measured using TM-align,[43] and the RMSD matrix was converted to a phylogenetic tree using the R package APE.[44]

■ ASSOCIATED CONTENT

Data Availability Statement
The data sets generated during and/or analyzed during the current study are available from the corresponding author on reasonable request.

ⓈⒾ Supporting Information
The Supporting Information is available free of charge at https://pubs.acs.org/doi/10.1021/acsomega.4c02517.

> MSA-based phylogenetic tree of all five dehalogenases DeHa1−5 and their amino acid sequences, sequence WebLogo plots of DeHa4 and DeHa2 in comparison with similar hydrolases, mass spectrometry (LC-QQQ) chromatograms of DeHa4-DFA reaction, pairwise sequence alignment of the *Delftia acidovorans* DeHa2 with the L-2-haloacid dehalogenase from *Pseudomonus* sp. YL, pairwise sequence alignment of the *Delftia acidovorans* DeHa4 with the fluoroacetate dehalogenase RPA1163, and size exclusion chromatography of purified DeHa1−5 (PDF)

■ AUTHOR INFORMATION

Corresponding Authors
Nancy Kelley-Loughnane − *Air Force Research Laboratory, Materials and Manufacturing Directorate, WPAFB, Ohio,*

United States 45433-7131; ⓞ orcid.org/0000-0003-2974-644X; Email: nancy.kelley-loughnane.1@us.af.mil
Patrick B. Dennis − *Air Force Research Laboratory, Materials and Manufacturing Directorate, WPAFB, Ohio, United States 45433-7131;* ⓞ orcid.org/0000-0002-9336-2144; Email: patrick.dennis.6@us.af.mil

Authors
Sanaz Farajollahi − *Air Force Research Laboratory, Materials and Manufacturing Directorate, WPAFB, Ohio, United States 45433-7131*
Nina V. Lombardo − *Air Force Research Laboratory, Materials and Manufacturing Directorate, WPAFB, Ohio, United States 45433-7131; UES a BlueHalo Company, Dayton, Ohio, United States 45432-1894*
Michael D. Crenshaw − *Air Force Research Laboratory, Materials and Manufacturing Directorate, WPAFB, Ohio, United States 45433-7131; UES a BlueHalo Company, Dayton, Ohio, United States 45432-1894*
Hao-Bo Guo − *Air Force Research Laboratory, Materials and Manufacturing Directorate, WPAFB, Ohio, United States 45433-7131; UES a BlueHalo Company, Dayton, Ohio, United States 45432-1894*
Megan E. Doherty − *Department of Biology, United States Air Force Academy, Colorado Springs, Colorado, United States 80840-5002*
Tina R. Davison − *Air Force Research Laboratory, Materials and Manufacturing Directorate, WPAFB, Ohio, United States 45433-7131; UES a BlueHalo Company, Dayton, Ohio, United States 45432-1894*
Jordan J. Steel − *Department of Biology, United States Air Force Academy, Colorado Springs, Colorado, United States 80840-5002*
Erin A. Almand − *Department of Biology, United States Air Force Academy, Colorado Springs, Colorado, United States 80840-5002*
Vanessa A. Varaljay − *Air Force Research Laboratory, Materials and Manufacturing Directorate, WPAFB, Ohio, United States 45433-7131; The Ohio State University, Infectious Diseases Institute, Columbus, Ohio, United States 43210-1132*
Chia Suei-Hung − *Air Force Research Laboratory, Materials and Manufacturing Directorate, WPAFB, Ohio, United States 45433-7131*
Peter A. Mirau − *Air Force Research Laboratory, Materials and Manufacturing Directorate, WPAFB, Ohio, United States 45433-7131;* ⓞ orcid.org/0000-0002-5210-4990
Rajiv J. Berry − *Air Force Research Laboratory, Materials and Manufacturing Directorate, WPAFB, Ohio, United States 45433-7131;* ⓞ orcid.org/0000-0001-6355-8667

Complete contact information is available at:
https://pubs.acs.org/10.1021/acsomega.4c02517

Author Contributions

■ REFERENCES

(1) Dolbier, W. R. Fluorine Chemistry at the Millennium. *J. Fluor. Chem.* **2005**, *126* (2), 157−163.

(2) Tong, W.; Huang, Q.; Li, M.; Wang, J. Enzyme-Catalyzed C−F Bond Formation and Cleavage. *Bioresour. Bioprocess.* **2019**, *6* (1), 46.

(3) Wang, J.; Sánchez-Roselló, M.; Aceña, J. L.; del Pozo, C.; Sorochinsky, A. E.; Fustero, S.; Soloshonok, V. A.; Liu, H. Fluorine in Pharmaceutical Industry: Fluorine-Containing Drugs Introduced to the Market in the Last Decade (2001−2011). *Chem. Rev.* **2014**, *114* (4), 2432−2506.

(4) Han, J.; Kiss, L.; Mei, H.; Remete, A. M.; Ponikvar-Svet, M.; Sedgwick, D. M.; Roman, R.; Fustero, S.; Moriwaki, H.; Soloshonok, V. A. Chemical Aspects of Human and Environmental Overload with Fluorine. *Chem. Rev.* **2021**, *121* (8), 4678−4742.

(5) Inoue, M.; Sumii, Y.; Shibata, N. Contribution of Organofluorine Compounds to Pharmaceuticals. *ACS Omega* **2020**, *5* (19), 10633−10640.

(6) Yue, Y.; Fan, J.; Xin, G.; Huang, Q.; Wang, J.; Li, Y.; Zhang, Q.; Wang, W. Comprehensive Understanding of Fluoroacetate Dehalogenase-Catalyzed Degradation of Fluorocarboxylic Acids: A QM/MM Approach. *Environ. Sci. Technol.* **2021**, *55* (14), 9817−9825.

(7) Jeschke, P. Latest Generation of Halogen-containing Pesticides. *Pest Manag. Sci.* **2017**, *73* (6), 1053−1066.

(8) Leeson, A.; Thompson, T.; Stroo, H. F.; Anderson, R. H.; Speicher, J.; Mills, M. A.; Willey, J.; Coyle, C.; Ghosh, R.; Lebrón, C.; Patton, C. Identifying and Managing Aqueous Film-Forming Foam-Derived Per- and Polyfluoroalkyl Substances in the Environment. *Environ. Toxicol. Chem.* **2021**, *40* (1), 24−36.

(9) Fenton, S. E.; Ducatman, A.; Boobis, A.; DeWitt, J. C.; Lau, C.; Ng, C.; Smith, J. S.; Roberts, S. M. Per- and Polyfluoroalkyl Substance Toxicity and Human Health Review: Current State of Knowledge and Strategies for Informing Future Research. *Environ. Toxicol. Chem.* **2021**, *40* (3), 606−630.

(10) Wackett, L. P. Nothing Lasts Forever: Understanding Microbial Biodegradation of Polyfluorinated Compounds and Perfluorinated Alkyl Substances. *Microb. Biotechnol.* **2022**, *15* (3), 773−792.

(11) Che, S.; Jin, B.; Liu, Z.; Yu, Y.; Liu, J.; Men, Y. Structure-Specific Aerobic Defluorination of Short-Chain Fluorinated Carboxylic Acids by Activated Sludge Communities. *Environ. Sci. Technol. Lett.* **2021**, *8* (8), 668−674.

(12) Yang, S.-H.; Shi, Y.; Strynar, M.; Chu, K.-H. Desulfonation and Defluorination of 6:2 Fluorotelomer Sulfonic Acid (6:2 FTSA) by *Rhodococcus Jostii* RHA1: Carbon and Sulfur Sources, Enzymes, and Pathways. *J. Hazard. Mater.* **2022**, *423*, No. 127052.

(13) Kurihara, T.; Esaki, N.; Soda, K. Bacterial 2-Haloacid Dehalogenases: Structures and Reaction Mechanisms. *J. Mol. Catal. B Enzym.* **2000**, *10* (1), 57−65.

(14) Seong, H. J.; Kwon, S. W.; Seo, D.-C.; Kim, J.-H.; Jang, Y.-S. Enzymatic Defluorination of Fluorinated Compounds. *Appl. Biol. Chem.* **2019**, *62* (1), 62.

(15) Huang, S.; Jaffé, P. R. Defluorination of Perfluorooctanoic Acid (PFOA) and Perfluorooctane Sulfonate (PFOS) by *Acidimicrobium Sp.* Strain A6. *Environ. Sci. Technol.* **2019**, *53* (19), 11410−11419.

(16) Sima, M. W.; Huang, S.; Jaffé, P. R. Modeling the Kinetics of Perfluorooctanoic and Perfluorooctane Sulfonic Acid Biodegradation by *Acidimicrobium Sp.* Strain A6 during the Feammox Process. *J. Hazard. Mater.* **2023**, *448*, No. 130903.

(17) Mehrabi, P.; Schulz, E. C.; Dsouza, R.; Müller-Werkmeister, H. M.; Tellkamp, F.; Miller, R. D.; Pai, E. F. Time-Resolved Crystallography Reveals Allosteric Communication Aligned with Molecular Breathing. *Science* **2019**, *365* (6458), 1167−1170.

(18) Miranda-Rojas, S.; Toro-Labbé, A. Mechanistic Insights into the Dehalogenation Reaction of Fluoroacetate/Fluoroacetic Acid. *J. Chem. Phys.* **2015**, *142* (19), No. 194301.

(19) Alexandrino, D. A. M.; Ribeiro, I.; Pinto, L. M.; Cambra, R.; Oliveira, R. S.; Pereira, F.; Carvalho, M. F. Biodegradation of Mono-, Di- and Trifluoroacetate by Microbial Cultures with Different Origins. *New Biotechnol* **2018**, *43*, 23−29.

(20) Trang, B.; Li, Y.; Xue, X.-S.; Ateia, M.; Houk, K. N.; Dichtel, W. R. Low-Temperature Mineralization of Perfluorocarboxylic Acids. *Science* **2022**, *377* (6608), 839−845.

(21) Kyzer, J. L.; Martens, M. Metabolism and Toxicity of Fluorine Compounds. *Chem. Res. Toxicol.* **2021**, *34* (3), 678−680.

(22) Proudfoot, A. T.; Bradberry, S. M.; Vale, J. A. Sodium Fluoroacetate Poisoning. *Toxicol Rev.* **2006**, *25* (4), 213−219.

(23) Wackett, L. P. Strategies for the Biodegradation of Polyfluorinated Compounds. *Microorganisms* **2022**, *10* (8), 1664.

(24) Harris, J. D.; Coon, C. M.; Doherty, M. E.; McHugh, E. A.; Warner, M. C.; Walters, C. L.; Orahood, O. M.; Loesch, A. E.; Hatfield, D. C.; Sitko, J. C.; et al. Engineering and Characterization of Dehalogenase Enzymes from *Delftia Acidovorans* in Bioremediation of Perfluorinated Compounds. *Synth. Syst. Biotechnol.* **2022**, *7* (2), 671−676.

(25) Harris, J.; Gross, M.; Kemball, J.; Farajollahi, S.; Dennis, P.; Sitko, J.; Steel, J. J.; Almand, E.; Kelley-Loughnane, N.; Varaljay, V. A. Draft Genome Sequence of the Bacterium *Delftia Acidovorans* Strain D4B, Isolated from Soil. *Microbiol. Resour. Announc.* **2021**, *10* (44), e00635.

(26) Jitsumori, K.; Omi, R.; Kurihara, T.; Kurata, A.; Mihara, H.; Miyahara, I.; Hirotsu, K.; Esaki, N. X-Ray Crystallographic and Mutational Studies of Fluoroacetate Dehalogenase from *Burkholderia Sp.* Strain FA1. *J. Bacteriol.* **2009**, *191* (8), 2630−2637.

(27) Chan, W. Y.; Wong, M.; Guthrie, J.; Savchenko, A. V.; Yakunin, A. F.; Pai, E. F.; Edwards, E. A. Sequence- and Activity-Based Screening of Microbial Genomes for Novel Dehalogenases. *Microb. Biotechnol.* **2010**, *3* (1), 107−120.

(28) Khusnutdinova, A. N.; Batyrova, K. A.; Brown, G.; Fedorchuk, T.; Chai, Y. S.; Skarina, T.; Flick, R.; Petit, A. P.; Savchenko, A.; Stogios, P.; Yakunin, A. F. Structural Insights into Hydrolytic

Defluorination of Difluoroacetate by Microbial Fluoroacetate Dehalogenases. *Febs J.* **2023**, *290* (20), 4966−4983.

(29) Chan, P. W. Y.; Yakunin, A. F.; Edwards, E. A.; Pai, E. F. Mapping the Reaction Coordinates of Enzymatic Defluorination. *J. Am. Chem. Soc.* **2011**, *133* (19), 7461−7468.

(30) Jumper, J.; Evans, R.; Pritzel, A.; Green, T.; Figurnov, M.; Ronneberger, O.; Tunyasuvunakool, K.; Bates, R.; Žídek, A.; Potapenko, A.; Bridgland, A.; Meyer, C.; Kohl, S. A. A.; Ballard, A. J.; Cowie, A.; Romera-Paredes, B.; Nikolov, S.; Jain, R.; Adler, J.; Back, T.; Petersen, S.; Reiman, D.; Clancy, E.; Zielinski, M.; Steinegger, M.; Pacholska, M.; Berghammer, T.; Bodenstein, S.; Silver, D.; Vinyals, O.; Senior, A. W.; Kavukcuoglu, K.; Kohli, P.; Hassabis, D. Highly Accurate Protein Structure Prediction with AlphaFold. *Nature* **2021**, *596* (7873), 583−589.

(31) Guo, H.-B.; Varaljay, V.; Kedziora, G.; Taylor, K.; Farajollahi, S.; Lombardo, N.; Harper, E.; Hung, C.; Gross, M.; Perminov, A. Accurate Prediction by AlphaFold2 for Ligand Binding in a Reductive Dehalogenase: Implications for PFAS (per-and Polyfluoroalkyl Substance) Biodegradation. *Sci. Rep.* **2023**, *13*, 4082.

(32) Berman, H. M.; Westbrook, J.; Feng, Z.; Gilliland, G.; Bhat, T. N.; Weissig, H.; Shindyalov, I. N.; Bourne, P. E. The Protein Data Bank. *Nucleic Acids Res.* **2000**, *28* (1), 235−242.

(33) Li, Y.-F.; Hata, Y.; Fujii, T.; Hisano, T.; Nishihara, M.; Kurihara, T.; Esaki, N. Crystal Structures of Reaction Intermediates Of l-2-Haloacid Dehalogenase and Implications for the Reaction Mechanism. *J. Biol. Chem.* **1998**, *273* (24), 15035−15044.

(34) Mehrabi, P.; Di Pietrantonio, C.; Kim, T. H.; Sljoka, A.; Taverner, K.; Ing, C.; Kruglyak, N.; Pomès, R.; Pai, E. F.; Prosser, R. S. Substrate-Based Allosteric Regulation of a Homodimeric Enzyme. *J. Am. Chem. Soc.* **2019**, *141* (29), 11540−11556.

(35) Berhanu, A.; Mutanda, I.; Taolin, J.; Qaria, M. A.; Yang, B.; Zhu, D. A Review of Microbial Degradation of Per- and Polyfluoroalkyl Substances (PFAS): Biotransformation Routes and Enzymes. *Sci. Total Environ.* **2023**, *859*, No. 160010.

(36) Kamachi, T.; Nakayama, T.; Shitamichi, O.; Jitsumori, K.; Kurihara, T.; Esaki, N.; Yoshizawa, K. The Catalytic Mechanism of Fluoroacetate Dehalogenase: A Computational Exploration of Biological Dehalogenation. *Chem. Eur. J.* **2009**, *15* (30), 7394−7403.

(37) Kurihara, T.; Yamauchi, T.; Ichiyama, S.; Takahata, H.; Esaki, N. Purification, Characterization, and Gene Cloning of a Novel Fluoroacetate Dehalogenase from *Burkholderia Sp*. FA1. *J. Mol. Catal. B Enzym.* **2003**, *23* (2), 347−355.

(38) Zhang, H.; Tian, S.; Yue, Y.; Li, M.; Tong, W.; Xu, G.; Chen, B.; Ma, M.; Li, Y.; Wang, J. Semirational Design of Fluoroacetate Dehalogenase *RPA1163* for Kinetic Resolution of α-Fluorocarboxylic Acids on a Gram Scale. *ACS Catal.* **2020**, *10* (5), 3143−3151.

(39) Steinegger, M.; Söding, J. MMseqs2 Enables Sensitive Protein Sequence Searching for the Analysis of Massive Data Sets. *Nat. Biotechnol.* **2017**, *35* (11), 1026−1028.

(40) Katoh, K.; Misawa, K.; Kuma, K.; Miyata, T. MAFFT: A Novel Method for Rapid Multiple Sequence Alignment Based on Fast Fourier Transform. *Nucleic Acids Res.* **2002**, *30* (14), 3059−3066.

(41) Crooks, G. E.; Hon, G.; Chandonia, J.-M.; Brenner, S. E. WebLogo: A Sequence Logo Generator. *Genome Res.* **2004**, *14* (6), 1188−1190.

(42) Kumar, S.; Stecher, G.; Li, M.; Knyaz, C.; Tamura, K. MEGA X: Molecular Evolutionary Genetics Analysis across Computing Platforms. *Mol. Biol. Evol.* **2018**, *35* (6), 1547.

(43) Zhang, Y.; Skolnick, J. TM-Align: A Protein Structure Alignment Algorithm Based on the TM-Score. *Nucleic Acids Res.* **2005**, *33* (7), 2302−2309.

(44) Paradis, E.; Claude, J.; Strimmer, K. APE: Analyses of Phylogenetics and Evolution in R Language. *Bioinformatics* **2004**, *20* (2), 289−290.